



New method for the synthesis of $\text{Al}_2\text{O}_3\text{--CaO}$ and $\text{Al}_2\text{O}_3\text{--CaO--CaCO}_3$ systems from a metallic precursor by the sol–gel route

Robert E. Przekop¹ · Piotr Marciniak¹ · Bogna Sztorch² · Agnieszka Czapiak¹ · Mikołaj Stodolny² · Agnieszka Martyła³

Received: 23 August 2017 / Revised: 10 April 2018 / Accepted: 26 April 2018 / Published online: 10 May 2018
© The Author(s) 2018

Abstract

A series of binary $\text{Al}_2\text{O}_3\text{--CaO}$ and $\text{Al}_2\text{O}_3\text{--CaO--CaCO}_3$ systems with Ca/Al molar ratios of 0.05, 0.1, 0.25, 0.5 and 1.0 have been synthesised by the sol–gel technique from aluminium isopropoxide and metallic calcium powder. The rate of the metal reaction is used as a limiting factor to control the binary gel formation. The proposed modification of the traditional sol–gel method was used to examine the influence the effect of the metallic form of the second component as an oxide precursor on the form of the final product. By applying acetic acid instead of mineral acid, calcium acetate is formed and then decomposed to calcium carbonate upon thermal processing. During the synthesis of the binary systems, metallic calcium acts both as a precursor of calcium acetate and as a secondary pH modifier of the gel system. Calcination in air at 600 °C did not produce systems containing only oxides and the calcium carbonate phase was still present. Due to particle size reduction, the CaCO_3 to CaO decomposition temperature was lowered. The systems were characterised by X-ray powder diffraction, low-temperature nitrogen adsorption, transmission and scanning electron microscopy (TEM, SEM and SEM/EDS), thermogravimetric analysis (TGA) and FTIR spectra.

Keywords CaO modified alumina · Alumina xerogel · Mixed oxide/carbonate phases · Sol-gel · Metallic precursor

Introduction

$\text{Al}_2\text{O}_3\text{--CaO}$ systems in the form of cement or oxides have excellent flame retardant qualities that are important from the point of view of industrial applications, e.g., for production of flooring, mortars resistant to chemicals and concretes, for construction of sewers, production of tile adhesives, or protective laminates [1–3]. Addition of CaO considerably improves the stability of the Pd/ Al_2O_3 catalyst by reducing carbon deposit formation and Al_2O_3 support transformation in

the catalytic reaction of partial oxidation of methane (POM). It also contributes to maintaining large surface area of the support [4]. $\text{Al}_2\text{O}_3\text{--CaO}$ system, thanks to its properties, can be used as high-temperature CO_2 absorbent [5] in the reforming process [6] or as an efficient adsorbent for fluorine removal from water [7]. Another field of application of this type of oxide is metallurgy. The CaO ability to bind to the non-metallic systems allows a better deoxidation of steel [8]. By careful selection of the key parameters of the gel synthesis and processing, including solvent type, precursor concentration, water and acid (or base) ratio, gel aging time, initial heat treatment and calcination, it is possible to control the process to obtain materials having properties suitable for a particular application [9]. These variables influence the process of gel network formation that determines the structure, physical properties, thermal stability, porosity and surface area of the xerogel [10, 11].

In this work, a new synthesis method has been proposed, in which calcium metal powder is used as alternative source of the second component of the gel matrix. Our previous work has shown that the introduction of a metal precursor could lead to a change in the parameters of the final product [12] and to the formation of new (carbonate) intermediate phases upon thermal treatment [13]. One of the goals of this

Electronic supplementary material The online version of this article (<https://doi.org/10.1007/s41779-018-0197-0>) contains supplementary material, which is available to authorized users.

✉ Robert E. Przekop
rprzekop@amu.edu.pl

¹ Centre for Advanced Technologies Adam Mickiewicz University in Poznan, Umultowska 89c, 61-614 Poznan, Poland

² Faculty of Chemistry, Adam Mickiewicz University in Poznan, Umultowska 89b, 61-614 Poznan, Poland

³ Central Laboratory of Batteries and Cells, Institute of Non-Ferrous Metals Division in Poznan, Forteczna 12, 61-362 Poznan, Poland

procedure was to maintain large initial surface area after modification, which is of importance for application of the systems as a carrier for metallic phase catalysts or for other purposes. The introduction of metallic calcium was a fast, pure and efficient method for incorporation of the second component of the alumina gel matrix. In addition, the replacement of mineral acids in the sol–gel synthesis, such as hydrochloric [14, 15], nitric [16, 17] or sulphuric acid [18], by acetic acid allows the formation of a carbonate form that is stable over a relatively wide temperature range.

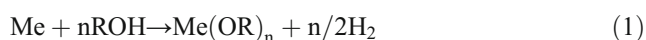
Materials and methods

Materials

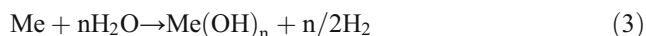
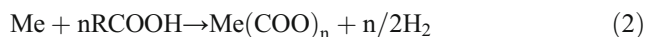
Aluminium isopropoxide ($\geq 98\%$), acetic acid ($\geq 99.5\%$) and metallic calcium (granular, 99%) were purchased from Sigma-Aldrich and used as received, without any further treatment.

Preparation

Al_2O_3 –CaO binary oxide systems of different molar ratios of Ca to Al: 0.05, 0.1, 0.25, 0.5 and 1.0 were synthesised by aqueous sol–gel chemistry. The synthesis was based on our previous experience with similar systems [12, 19, 20] but with a novel synthesis modification concerning the source of the second oxide component of the system. Synthesis of oxide systems based on the sol–gel method is based primarily on the use of metal alkoxides as precursors, while the methods for obtaining metal alkoxides often employ a direct reaction of metal (mainly of an alkaline nature) with the corresponding alcohol according to the reaction:



In the proposed method of synthesis, apart from the hydrolysis and condensation reactions of the alumina precursor, direct reactions of metallic calcium in a system containing acid (2) and water (3) have the dominant role, giving respectively acetate and hydroxide, which undergo further reactions.



Aluminium isopropoxide was used as a precursor of the starting alumina, while acetic acid was applied as a moderator of hydrolysis and condensation rates (regulation of pH). The reaction took place in a 2-l glass reactor upon stirring under reflux. The precursor of alumina (100 g of fine powder) was slowly added and hydrolysed in 880 cm^3 of water at 75 °C and after 2 h of stirring, the resulting slurry was peptized with 35 g (33.5 cm^3) of glacial acetic acid. In all preparations, the molar

ratio of $\text{Al}(\text{C}_3\text{H}_7\text{O})_3$, water and acetic acid was constant and equal to 1:100:1.2. The sol was refluxed for more than 24 h at 95 °C (Fig. 1).

After that time, an appropriate amount of metallic calcium in the form of granules was added in small portions as the second oxide component precursor. Table 1 shows sample labelling, composition and the amount of calcium added to each oxide system (per 100 g of aluminium isopropoxide).

The resulting mixture was refluxed upon vigorous stirring for 18 h at 95 °C. The final product was a homogeneous, liquid gel. The gel was poured onto the Petri dish and dried at 65 °C for 72 h to obtain a monolithic xerogel used for further TG investigation.

For wet gels up to the Ca/Al 0.5 system, a high degree of homogeneity was obtained after synthesis (Fig. 2a) but for the 1.0 system (with the highest Ca content), the result of phase segregation can be seen (Fig. 2a). This is also reflected in morphological parameters and textural properties. Gel drying reveals differences in their homogeneity already in macroscopic terms. Gels of lower Ca content systems, Ca/Al 0.1, 0.25 (Fig. 1b), remain transparent, and for higher concentrations, their turbidity or clear crystallisation is visible (Ca/Al 1.0). The obtained gel was evaporatively dried (90 °C, 80 mbar) and the resulting solid was ground in a mortar; sieved to collect two required grain fractions, 0.1–0.2 mm and <0.1 mm; and annealed at 600 °C in air flow for 6 h. For the porous structure determination, the grain size fraction between 0.1 and 0.2 mm of diameter was used. For the XRD and electron microscope analysis, the latter fraction was used.

Characterisation

The samples synthesised in this work were characterised using the following techniques.

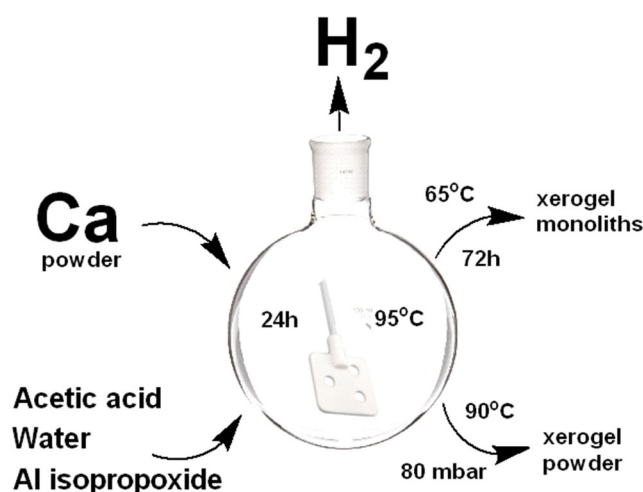


Fig. 1 Schematic procedure of Ca/Al gel synthesis

Table 1 Composition and labelling of the systems and the amount of added metallic calcium

Sample name	Al ₂ O ₃	Ca/Al 0.05	Ca/Al 0.1	Ca/Al 0.25	Ca/Al 0.5	Ca/Al 1.0
Relative molar amount of Al	1	1	1	1	1	1
Relative molar amount of Ca	0	0.05	0.10	0.25	0.50	1
Mass of added Ca [g]	0	0.98	1.96	4.90	9.80	19.59

X-ray powder diffraction analysis

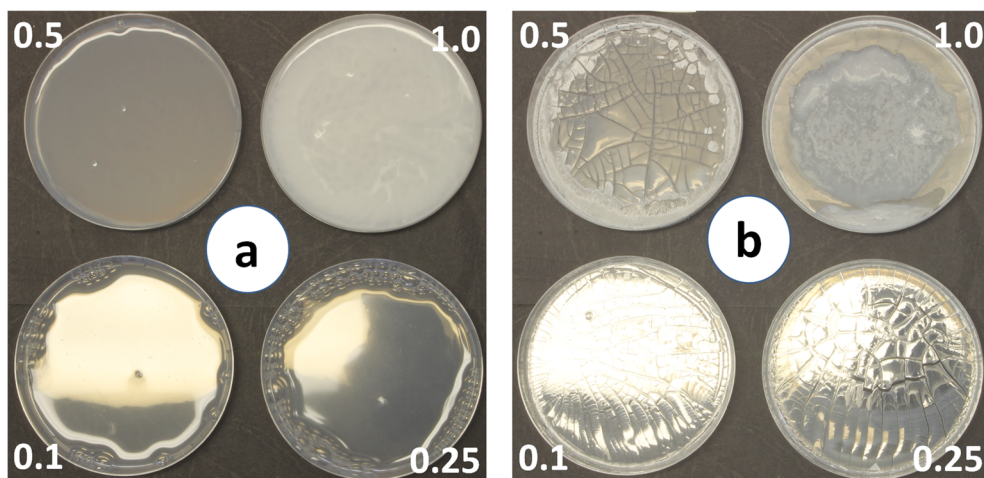
The X-ray powder diffraction (XRPD) measurements were carried out using a Philips PW1050 diffractometer working in the θ - 2θ geometry with Ni-filtered CuK α radiation. The following measurement conditions were applied: 2θ 5–100°, voltage 35 kV, current 20 mA, scan step 0.040° at 1° per minute. The positions of reflections were calculated by the Philips APD program.

Thermal analysis

Thermal transformation of unprocessed gel samples was carried out on a NETZSCH TG 209 F1 Libra thermogravimetric apparatus. A 5-mg sample was placed in an alumina crucible (85 μ l volume) and heated at a rate of 20 °C min⁻¹ up to 1000 °C. For all experiments, the fraction of the grain size below 0.1 mm was used. The TG traces were recorded in air atmosphere (20 ml/min flow) with a resolution of 0.1 μ g. No drying under vacuum or at elevated temperature was applied.

SEM, TEM and EDS (energy-dispersive X-ray spectroscopy) analysis

Surface morphology of the oxide systems was depicted by a scanning electron microscope (Quanta 250 FEG scanning electron microscope) which was operated at 5 kV) with EDAX system for EDS analysis, and their structures were characterised by transmission electron microscopy (JEOL 200 CX which was operated at 80 kV). EDS maps of element overlay were made with a resolution of 0.3 μ m.

Fig. 2 Gel photos before (a) and after drying at 65 °C, 24 h (b)

Porous structure

The porous structure was determined by the low-temperature nitrogen adsorption measurements carried out on an Autosorb iQ Station 2 (Quantachrome Instruments) in standard analysis mode, using 200–300 mg of material with the grain size fraction between 0.1 and 0.2 mm. Prior to nitrogen adsorption, all samples were outgassed for about 10 h at 350 °C at 0.4 Pa till constant weight. Both adsorptive and desorptive branches of the isotherm were recorded in the range of p/p_0 0–1.0. Reports were provided by Quantachrome ASiQwin software (version 2.0). Distribution of pore area and pore volume was calculated using the de Boer t-method and BJH method. Pore volume and pore diameter were found from the adsorptive branch of the isotherm using the BJH method, and surface area was calculated using the BET method.

FTIR measurements

FTIR measurements were carried out using a Thermo Scientific Nicolet iS50 FTIR spectrometer. One milligram was mixed with 200 mg KBr and pressed at 10 t press into the form of discs.

Results and discussion

Modification of alumina gel network employing a metallic precursor of calcium oxide may have numerous implications. It is known that the reactivity of alkoxide precursor can be changed and controlled by various parameters, such as the type and

Table 2 Values of pH of the gels after synthesis

System composition	pH
Al ₂ O ₃ [Al(O)OH]	3.39
Ca/Al 0.05	4.11
Ca/Al 0.1	4.64
Ca/Al 0.25	5.25
Ca/Al 0.5	6.06
Ca/Al 1.0	10.25

concentration of precursor, temperature, water and acid or base content, solvent type. Also, other parameters related to further steps of preparation influence the gel forming process: gel ageing time and drying method [12, 21]. In this process, thanks to its strong basicity, calcium can act as a pH regulator and therefore can significantly affect the further process of solid gel formation and transformation, also upon drying and annealing.

The rate of reaction of metallic calcium granules (in comparison to other precursors) with gel solution may be an obstacle to proper process control and result in heterogeneities. Also, the proposed method employing metallic calcium was used as an alternative to traditional methods of co-precipitation (e.g., of carbonates) or carrier impregnation with salts (e.g., nitrates) which often lead to a considerable decrease in the carrier surface area.

Table 2 shows the pH values of the gels after the synthesis. With the addition of calcium, the acidity of the solution decreases continuously in a series of samples and their pH increases to a high value for the Ca/Al 1.0 system. The pH of the solution changes the net surface charge of sol particles that depends on the point of zero charge of the oxide components. Alumina particles are charged negatively at the pH higher than the PZC of γ -Al₂O₃ ($pH_{PZC} = 8.2$ [7], but also values 6.2 to 7.9 have been

reported [22] and have been reported γ -Al(O)OH pH_{PZC} values of ca. 7.4 [22]) and can attract positively charged calcium species in a basic solution.

X-ray powder diffraction

The XRPD patterns of the samples after the synthesis (before calcination) are shown in Fig. 3a. The presence of crystalline phases of Ca(OH)₂, bohemite and calcium acetate was identified in the samples; they disappear after calcination and thermal decomposition of precursors [23].

The calcined samples (6 h at 600 °C under continuous oxygen flow) are amorphous and only minor amounts of any crystalline phases have been found in them (Fig. 3b). After thermal treatment, the intensity of the diffraction peaks decreases with increasing content of calcium oxide and only a wide peak assigned to the low-crystallinity γ -Al₂O₃ phase in the range of $2\theta = 20$ – 40° is observed [7] with small single peaks of CaCO₃ and CaO crystalline phase for the systems Ca/Al 0.25 to 1.0.

The positions of two broad maxima suggest that the system Ca/Al 0.05 contains higher amount of low-crystallinity γ -Al₂O₃ phase. This effect is diminished in further compositions, not only because of the lower content of this component but also as a result of interaction with the calcium phase. However, after calcination in air at 600 °C, the calcium carbonate phase was still present. This fact can be explained by the use of acetic acid during the synthesis and formation of calcium acetate that is transformed into carbonate, and its decomposition to CaO requires higher temperature. Depending on the calcination temperature, the systems Al₂O₃–Ca(CH₃COO)₂ (< 320 °C), Al₂O₃–CaCO₃ (430–650 °C) or Al₂O₃–CaO (> 700 °C) can be obtained in the same way.

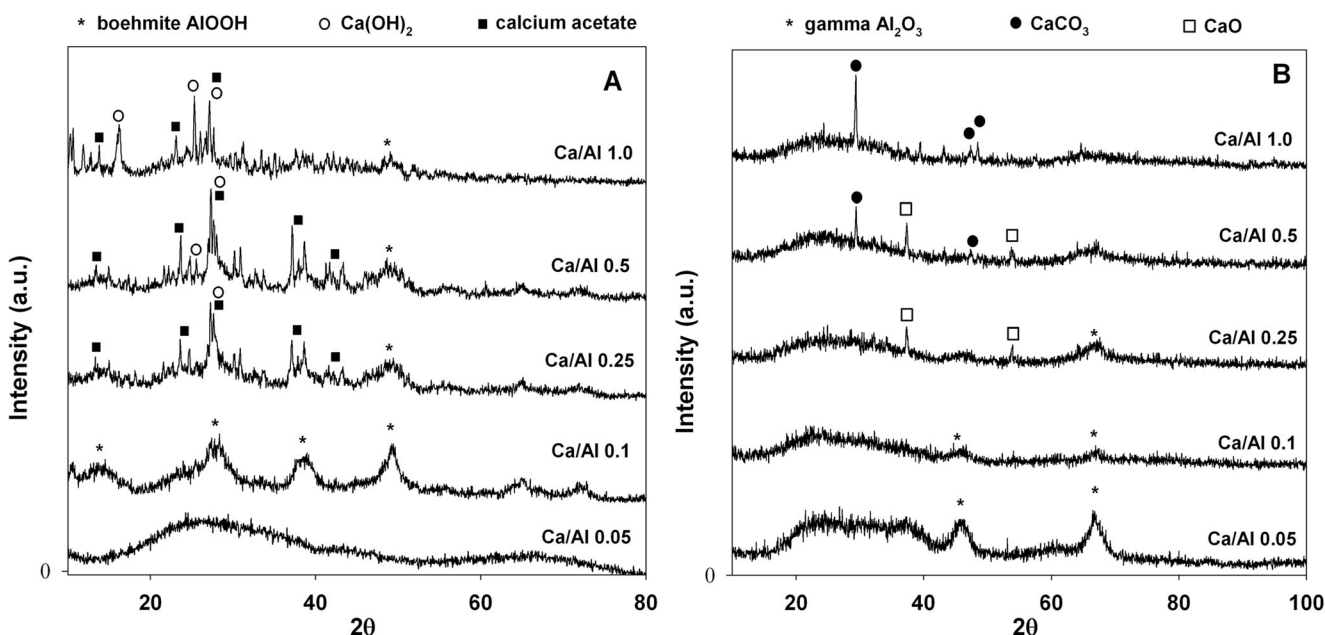
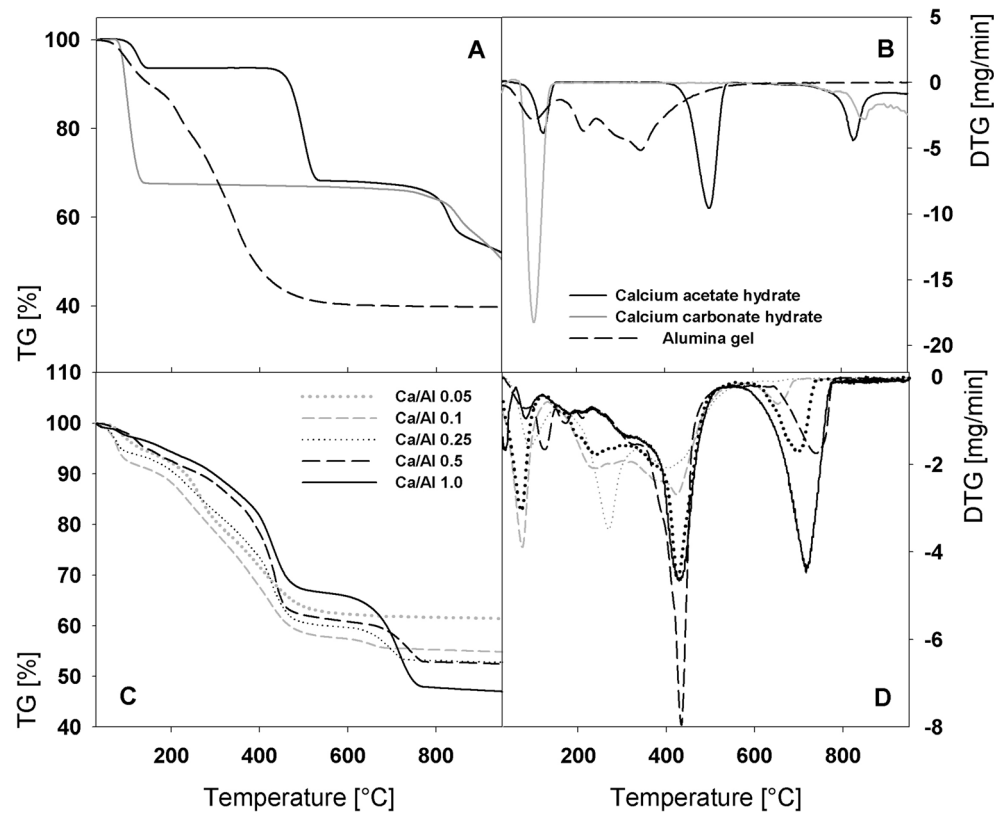


Fig. 3 XRPD patterns of Ca/Al systems: **a** before calcination and **b** after calcination at 600 °C in oxygen atmosphere

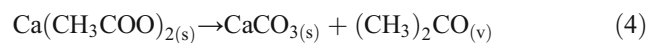
Fig. 4 Thermogravimetric analysis of Ca/Al systems. **a** TG traces of reference materials. **b** DTG traces of reference materials. **c** TG traces of Ca/Al systems. **d** DTG traces of Ca/Al systems



Thermal analysis

Thermograms of the analysed systems are shown in Fig. 4. For alumina gel, three characteristic areas of mass loss effects are observed. They are related to the dehydration, dehydroxylation and oxidation process of organic compounds bound to the gel structure (Fig. 4a). On the basis of previous works [12, 21], the first endothermic mass loss was interpreted as corresponding to the removal of physisorbed and internally trapped water in gel. This effect is responsible for the loss of < 10% of the total weight of the gel dried at room temperature. As a result of further heating, the decomposition and desorption of the organic compounds combined with their oxidation follows. This exothermic effect occurs in the temperature range of 390–530 °C (range (III), Table 3). Also, Ca(OH)₂ is decomposed to CaO (Fig. 3 XRPD patterns).

With respect to the undoped Al₂O₃, the obtained binary oxide systems do not exhibit a higher complexity of thermal decomposition and desorption processes. As the calcium content increases, the thermograms become similar to the calcium acetate thermal profile (Fig. 4b). In the temperature range of 370–570 °C, the dominant transformation is the decomposition of calcium acetate according to the equation [24]:



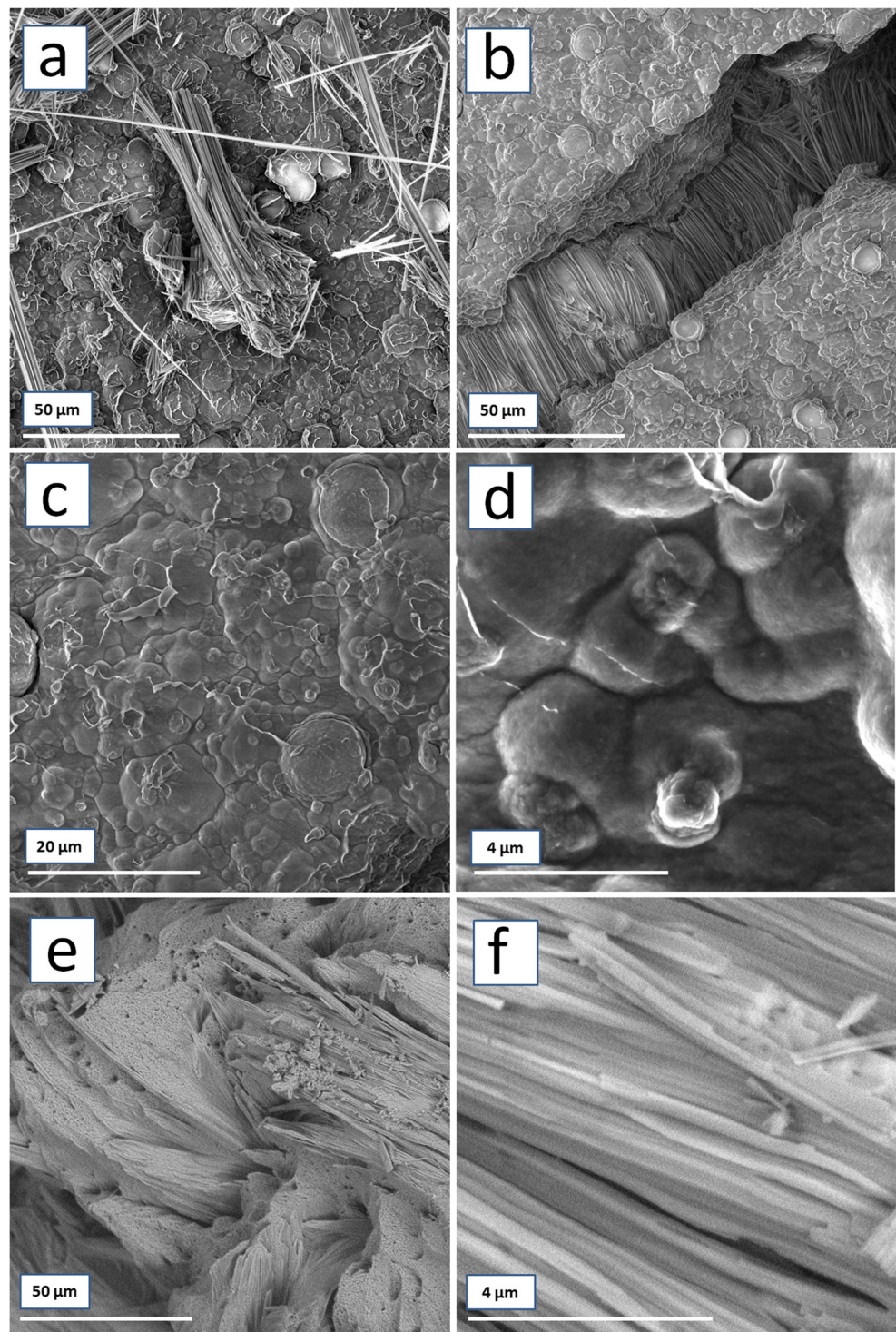
In this temperature range (III), also calcium hydroxide undergoes decomposition (> 512 °C). Above 680 °C, an additional weight loss associated with the decomposition of calcium carbonate takes place:



Table 3 Quantitative mass loss of the Ca/Al systems during thermogravimetric analysis

System composition	Ca/Al 0.05	Ca/Al 0.1	Ca/Al 0.25	Ca/Al 0.5	Ca/Al 1.0
Temperature range [°C]	Sample mass loss [%]				
I 30–200	6.25	9.1	9.3	7.41	5
II 200–370	13	11.8	13.8	8.6	8.42
III 370–570	16.9	20.38	17	22	20.4
IV 570–800	2	3.45	6.7	9.2	18.8
Total mass loss	38.15	44.73	46.8	47.21	52.62

Fig. 5 SEM micrographs of Ca/Al gel monoliths before calcination at the Al/Ca molar ratio: **a** 0.1, **b–d** 0.25, **e, f** 1.0



Both effects (III, IV) are shifted to lower temperatures (430 and 720 °C) when compared to that for the reference substances and literature data (500 and 810 °C) [25]. This is an effect of particle size reduction [26]. In quantitative terms, the process of gel decomposition after its synthesis results in more volatile degradation products with increasing calcium content. The most important difference from

the other methods for the synthesis of binary oxide systems based on an alumina matrix is the fact that a stable calcium carbonate phase is obtained in the range 500–630 °C. The above observations are confirmed by spectroscopic analysis of structural bands in the range 1600–400 cm^{-1} . It is worth noting that Al_2O_3 and CaO have no catalytic effect on the kinetics of CaCO_3 calcination [26].

SEM, TEM and EDS analyses

The SEM micrographs of the uncalcined samples' surfaces (Fig. 5) show the formation of two distinct phases during gelation: the amorphous phase of alumina/calcium acetate (Fig. 5a–d) consisting of densely packed spherical domains of different size (Ca/Al 0.1 system: mainly approximately 10 μm and small amount of ca. 0.25 μm) and microcrystalline phase of calcium acetate forming bundles of long ($\sim 25 \mu\text{m}$), thin (ca. 50 nm), parallel fibres (Fig. 5a, b, e) present in the structure of the material before and after thermal treatment [26]. The formation of the two phases is independent of the calcium to aluminium ratio (Fig. 5a–f). Another significant observation is the formation of a calcium acetate-rich phase under the surface of the alumina enriched phase (Fig. 5b). The EDS elemental analysis of the surface also shows the presence of two phases (Fig. 6).

The SEM micrographs of the materials with higher calcium content after calcination at 600 $^{\circ}\text{C}$ show two phases (Fig. 7a–c) as observed for the samples before calcination (Fig. 5). The calcination changes the structure of alumina transforming it into a smooth, continuous and amorphous phase (Fig. 7a), but the calcium carbonate phase remains structurally similar to the calcium acetate phase. The surface texture of the two calcined systems is typical of alumina (Fig. 7a) yet very different for high calcium content (Fig. 7b) that is less porous, and the microcrystalline calcium carbonate phase is present. For the Ca/Al 0.1

system, the ratio of Ca to Al obtained from the EDS map of uncalcined systems is more than twice (0.25) higher than that resulting from the theoretical composition and indicates the concentration of calcium ions on the surface as well as for the systems Ca/Al 0.25 (Ca/Al = 0.49) and Ca/Al 0.5 (Ca/Al = 0.74). For the Ca/Al 1.0 system, the ratio of Ca to Al is many times higher and equal to 43, which points to the almost complete coverage of the surface layer with calcium precursor (acetate). Thus, the binary systems are not fully homogeneous but they are also microcrystalline or highly amorphous. The location and orientation of the two phases is not clear: EDS data suggest increasing effect of alumina surface decoration with calcium component; however, SEM images indicate the presence of the latter component under alumina surface or between layers and planes of the alumina matrix.

Figure 8 shows TEM micrographs of calcined samples. The amorphous alumina structure is visible, but it is difficult to indicate the presence of the calcium phase, which is separated from the Al_2O_3 matrix and should be visible as “rods” of CaO crystals.

Porous structure—low temperature nitrogen adsorption–desorption

Surface area, pore volume and pore diameter are presented in Table 4. Plots of isotherms, pore volume distribution and pore area distribution are shown in Fig. 9.

Fig. 6 EDS elements maps of Ca/Al gel monoliths before calcination at the Al/Ca molar ratio: **a** 0.1, **b** 0.25, **c** 0.5, **d** 1.0

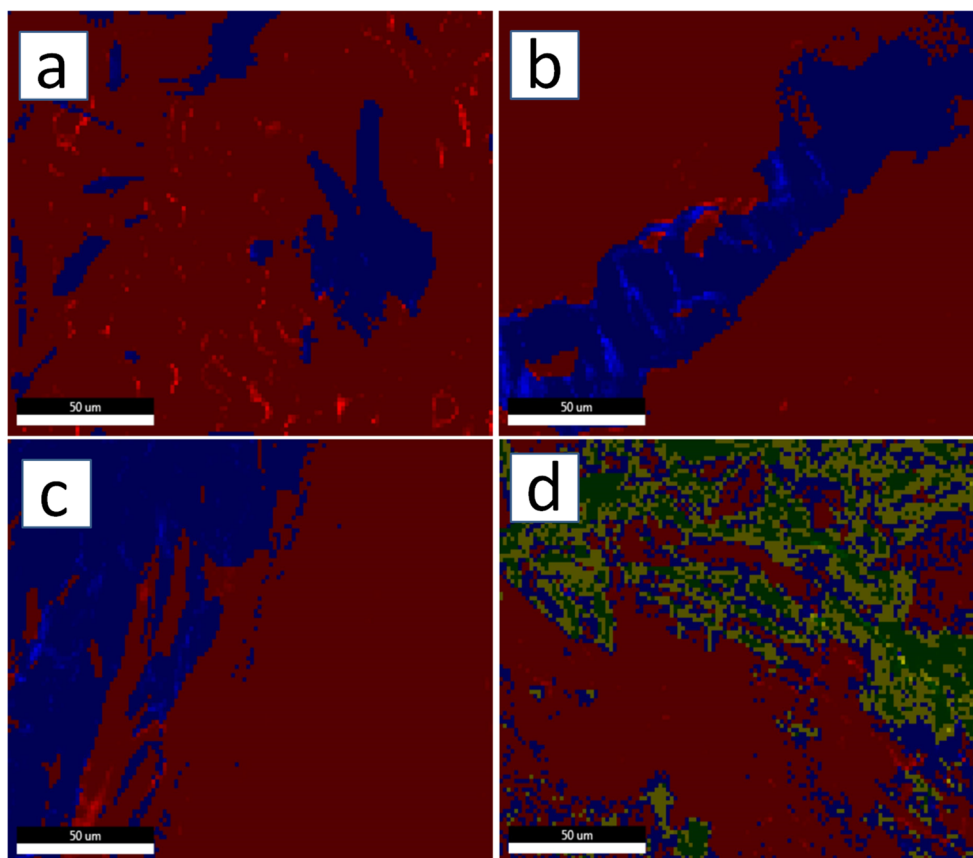
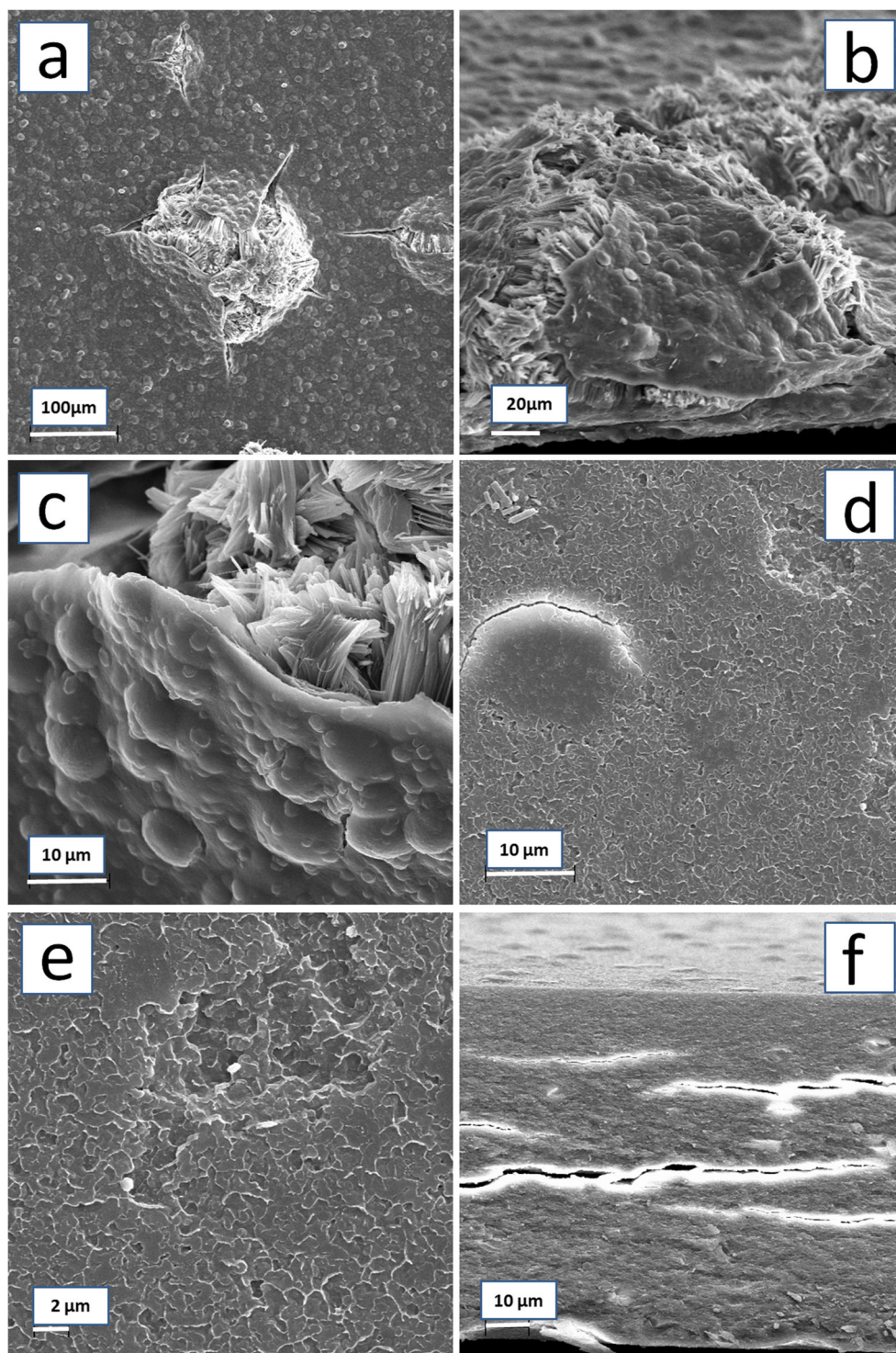


Fig. 7 SEM micrographs of Ca/Al samples calcined at 600 °C at the Al/Ca molar ratio: **a–c** 1.0, **d–f** 0.25



Binary systems based on alumina in a wide range of CaO content have large surface area ($\sim 180\text{--}320\text{ m}^2/\text{g}$), which decreases almost linearly with the content of the second component (having much lower specific surface area) to about $70\text{ m}^2/\text{g}$ for the Ca/Al 1.0 system. The adsorption–desorption isotherm is type IV with H2 hysteresis loop (except for the Ca/Al 0.05 system) that is found in the range of relative pressure

p/p_0 0.5–1, which is characteristic of metal oxide mesoporous materials. The shape of hysteresis loops is similar for the oxides with Ca/Al ratio higher than 0.05. The obtained systems contain mainly small mesopores ($< 10\text{--}15\text{ nm}$) which bring the largest contribution to the surface area. The average pore size remains constant at about 6 nm, and the pore size distribution is narrow.

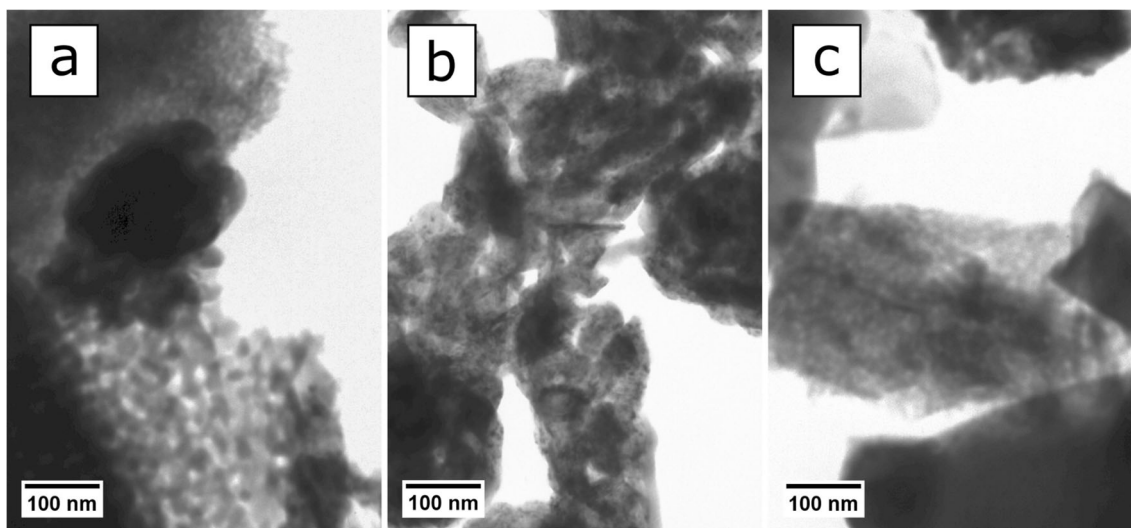


Fig. 8 TEM images of Ca/Al sol-gel samples at the Al/Ca molar ratio: **a** 0.1, **b** 0.5, **c** 1.0

The texture of Ca/Al 0.05 system is the most distinctive. In addition to small mesopores (average diameter of about 3 nm) resulting from high alumina content, some larger mesopores are present, including the ones in the range of 10–20 nm in diameter. This is particularly evident taking into account the surface area and volume distribution curves obtained from the desorptive branch of the isotherm and the shape of isotherms and the hysteresis loop. However, the addition of calcium component causes the disappearance of the smallest pores in favour of larger mesopores. Their size and distribution does not change significantly with its amount. Multi-modal distribution of pores suggests complex and not fully homogenous structure of the system. The pore volume of the systems decreases from 0.65 to 0.17 cm³/g with increasing calcium content, similarly to the changes in the surface area. The highest pore volume of the Ca/Al 0.05 system is associated with a significant volume of larger mesopores having a diameter of about 15 nm, whose presence is also apparent from the H2/H3 mixed-type hysteresis loop of nitrogen adsorption isotherm. For this sample, it is even higher than for unmodified alumina. Despite the fact that the decrease in pore volume may be caused by CaO or CaCO₃ particles located in pores of alumina

(blockage of pores) [7], it can be assumed that this decrease is mostly the effect of alumina surface coverage with calcium component, as suggested by the results of EDS element mapping. The H3-type hysteresis loop observed at high values of p/p_0 indicates the presence of plate-like particle aggregates, giving rise to the slit-shaped pores in which the capillary condensation occurs, in addition to bottle-shaped pores with narrow necks (the H2 type hysteresis loop) [27]. For all alumina-based systems, a moderate negative effect of CaO addition on the surface area and pore volume can be observed, with little impact on their average diameter and distribution. The increase in CaO/CaCO₃ content also causes disappearance of the smallest pores.

FTIR measurements

Spectroscopic studies have provided information on the composition of the obtained systems after sol-gel synthesis and after calcination (Fig. 10). Uncalcined samples show characteristic intense bands assigned to asymmetric and symmetric vibrations of calcium acetate carboxylate groups in the range of 1612–1350 cm⁻¹. After calcination, as a result of calcium acetate

Table 4 Textural properties of Ca/Al systems

System composition	Surface area S _{BET} [m ² /g]	Average pore diameter D _{BJH} [nm]	Average pore volume D _{BJH} [cm ³ /g]
Al ₂ O ₃ ^a	337.2	5.5	0.49
Ca/Al 0.05	322.0	3.3	0.65
Ca/Al 0.1	272.7	5.8	0.45
Ca/Al 0.25	233.0	5.8	0.42
Ca/Al 0.5	179.0	6.3	0.33
Ca/Al 1.0	67.9	6.8	0.17

^a From reference [12]

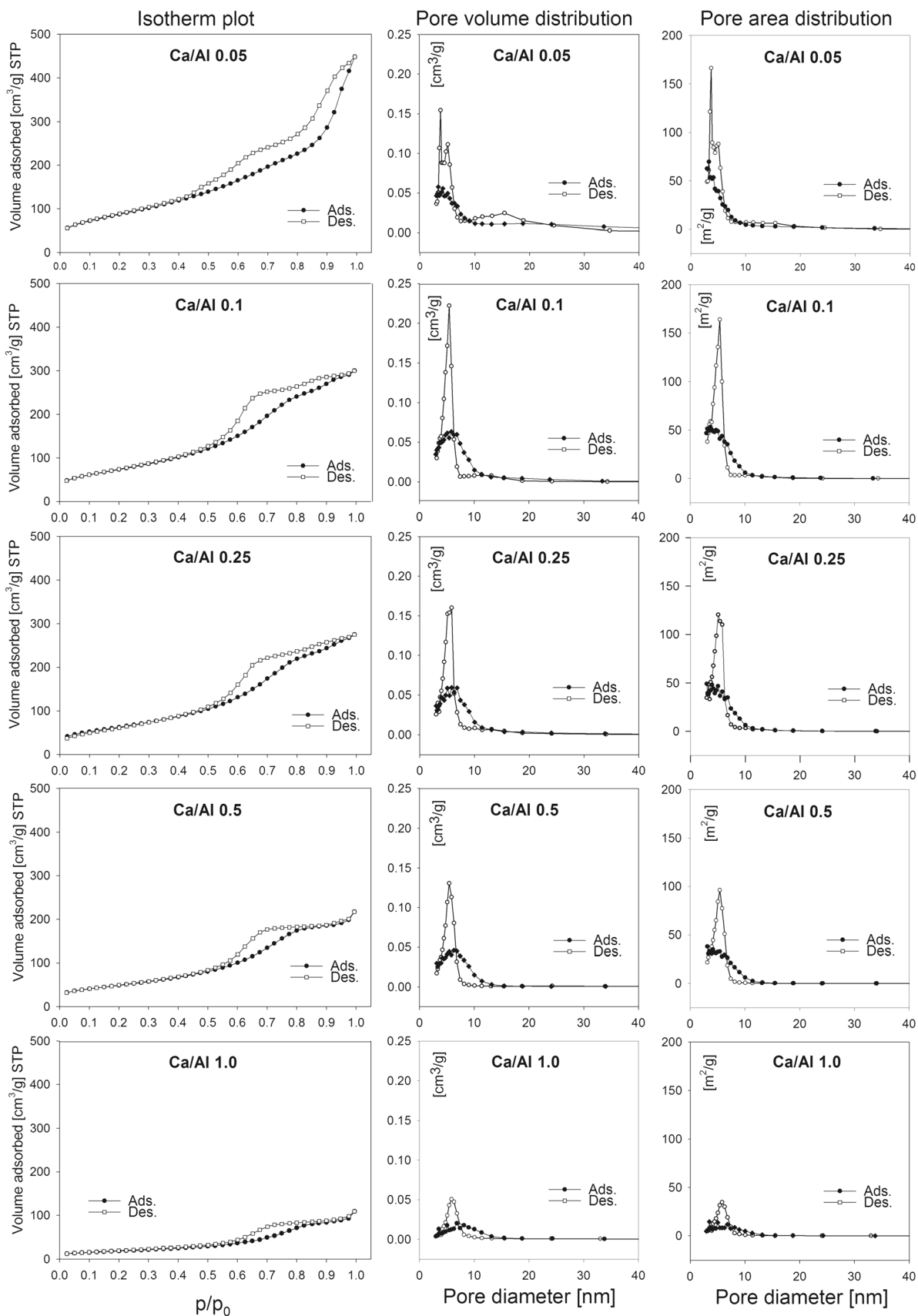


Fig. 9 Isotherms, pore volume distribution and pore area distribution of the Ca/Al systems

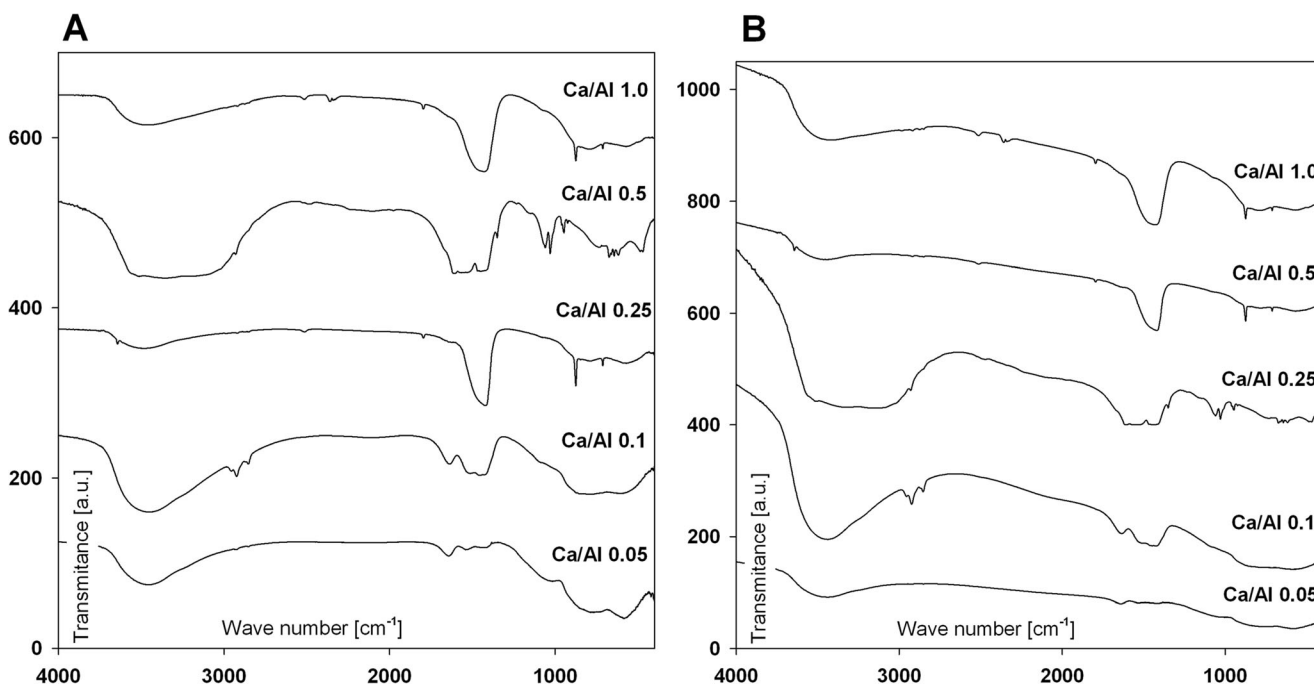


Fig. 10 FTIR spectra of Ca/Al systems. **a** Before calcination. **b** After calcination

decomposition, the bands disappeared and broad intense bands assigned to symmetric stretching vibration of unidentate carbonate at 1540 cm^{-1} appeared [28]. No bridged bidentate carbonate ($1620\text{--}1670\text{ cm}^{-1}$) was found. Also, the appearance of a sharp band at 875 cm^{-1} , assigned to the carbonate ionic group (CO_3^{2-}), confirms the presence of calcium carbonate after thermal treatment [29]. The carbonate bands are observed for the Ca/Al 0.25, 0.5 and 1.0 systems. A clear 1166 cm^{-1} band assigned to the octahedral Al is visible for uncalcined systems [25] and diminishes with increasing calcium content. This band disappears after calcination. For low calcium contents, a weak Al–OH band (1640 cm^{-1}) shifted to low-frequency occurs, which vanishes with decreasing of Ca content [30].

Conclusions

The rate of the reaction of metallic calcium with alumina precursor solution has a limited effect on the structure and homogeneity of the oxides systems. We assume that in these systems, the pH increase related to the calcium content is a determining parameter of alumina gel formation [9, 21]. Both components form a mixture of two separate phases: amorphous alumina and crystalline CaCO_3/CaO . The surface properties of the mixed $\text{Al}_2\text{O}_3\text{--CaO}$ systems are largely influenced by the CaO and CaCO_3 phases which have a clear tendency to concentrate on alumina surface in the crystalline form and presumably, they also cause pores blockage, which can be evidenced by disappearance of larger pores. It is visible from the textural data

analysed in combination with microscopic images. High CaCO_3/CaO content, because of decreasing ratio of Al/Ca, is responsible for a significant, almost linear decrease in the specific surface area and pore volume. Introduction of calcium component to alumina matrix, as seen from the XRPD patterns, results in stabilisation of dispersion of the binary systems and decreases the transformation of amorphous alumina into the $\gamma\text{-Al}_2\text{O}_3$ crystalline phase. The Ca/Al 0.05 composition has distinctly different structural and surface properties, similar to those of undoped Al_2O_3 obtained by the sol–gel method. Application of the sol–gel route allows obtaining a highly dispersive but not strictly homogeneous system irrespective of the molar ratio of the components. The dispersion and homogeneity of the system diminishes with the rising calcium content in the system. Acetic acid used as a reagent and pH regulator allows the formation of various chemical forms of calcium in the alumina matrix: acetate, carbonate or oxide in the structure of the material. Their formation translates into the final properties of the products, e.g. texture or acid–base properties.

Compliance with ethical standards

Conflict of interest The authors declare that they have no conflict of interest.

Open Access This article is distributed under the terms of the Creative Commons Attribution 4.0 International License (<http://creativecommons.org/licenses/by/4.0/>), which permits unrestricted use, distribution, and reproduction in any medium, provided you give appropriate credit to the original author(s) and the source, provide a link to the Creative Commons license, and indicate if changes were made.

References

- Wang, Y., Diamond, S.: An approach to quantitative image analysis for cement pastes. *Mater. Res. Soc. Symp. Proc.* **370**, 23–32 (1995)
- Sohn, D., Mason, T.O.: Electrically induced microstructural changes in Portland cement pastes. *J. Adv. Cem. Based Mater.* **7**, 81–88 (1998)
- Schwartz, L.M., Garboczi, E.J., Bentz, D.P.: Interfacial transport in porous media: application to DC electrical conductivity of mortars. *J. Appl. Phys.* **78**, 5898–5908 (1995)
- Wang, J., Yu, H., Ma, Z., Zhou, S.: Enhanced stability of CaO and/or La₂O₃ promoted Pd/Al₂O₃ egg-shell catalysts in partial oxidation of methane to syngas. *Molecules.* **18**, 8289–8297 (2013)
- Zhao, C., Zhou, Z., Cheng, Z.: Sol-gel-derived synthetic CaO-based CO₂ sorbents incorporated with different inert materials. *Ind. Eng. Chem. Res.* **53**, 14065–14074 (2014)
- Wu, S.F., Li, Q.H., Kim, J.N., Yi, K.B.: Properties of a nano CaO/Al₂O₃ CO₂ sorbent. *Ind. Eng. Chem. Res.* **47**, 180–184 (2008)
- Dayananda, D., Sarva, V.R., Prasad, S.V., Arunachalam, J., Ghosh, N.N.: Preparation of CaO loaded mesoporous Al₂O₃: efficient adsorbent for fluoride removal from water. *Chem. Eng. J.* **248**, 430–439 (2014)
- Miskufova, A., Havlik, T., Koppelhuber-Bitschnau, B., Kielski, A., Pomadowski, H.: Properties of CaO sintered with addition of active alumina. *Ceramics-Silikáty.* **59**, 115–124 (2015)
- Suh, D.J., Park, T.J.: Sol-gel strategies for pore size control of high-surface-area transition-metal oxide aerogels. *Chem. Mater.* **8**, 509–513 (1996)
- Przekop, R., Kirszensztejn, P.: Porous xerogel systems B₂O₃–Al₂O₃ obtained by the sol–gel method. *J. Non-Cryst. Solids.* **402**, 128–134 (2014)
- Rezgui, S., Gates, B.C., Burkett, S.L., Davis, M.E.: Chemistry of sol-gel synthesis of aluminum oxides with in situ water formation: control of the morphology and texture. *Chem. Mater.* **6**, 2390–2397 (1994)
- Kirszensztejn, P., Przekop, R., Szymkowiak, A., Maćkowska, E., Gaca, J.: Preparation of MgO–Al₂O₃ binary gel system with mesoporous structure. *Microporous Mesoporous Mater.* **89**, 150–157 (2006)
- Przekop, R., Marciniak, P., Sztorch, B., Czapik, A., Stodolny, M., Martyla, A.: One-pot synthesis of Al₂O₃–La₂O₃CO₃ systems obtained from the metallic precursor by the sol-gel method. *J. Non-Cryst. Solids.* **479**, 105–112 (2018)
- Song, K.C., Chung, I.J.: The structure formations of aluminum hydroxide gels under HCl and NH₄OH conditions. *J. Non-Cryst. Solids.* **108**, 37–44 (1989)
- Feinle, A., Elsaesser, M.S., Hüsing, N.: Sol–gel synthesis of monolithic materials with hierarchical porosity. *Chem. Soc. Rev.* **45**, 3377–3399 (2016)
- Takeda, Y., Hashimoto, T., Nasu, H., Kamiya, K.: Crystallization behaviour of alumina gels prepared by sol-gel method using nitric acid as a catalyst—complete α -transformation at 800°C. *J. Ceram. Soc. Jpn.* **110**, 1025–1028 (2002)
- Kamiya, K., Hioki, N., Hashimoto, T., Nasu, H.: Formation of α -alumina around 500°C in alkoxy-derived alumina gels under ambient pressure—effects of starting solution composition and seeding. *J. Sol-Gel Sci. Technol.* **20**, 275–285 (2001)
- Temel, T.M., Ikizler, B.K., Terzioglu, P., Yücel, S., Elalimış, Y.B.: The effect of process variables on the properties of nanoporous silica aerogels: an approach to prepare silica aerogels from biosilica. *J. Sol-Gel Sci. Technol.* **84**, 51–59 (2017)
- Kirszensztejn, P., Szymkowiak, A., Marciniak, P., Martyla, A., Przekop, R.: Texture of Al₂O₃–SnO₂ binary oxides system obtained via sol-gel chemistry. *Appl. Catal. A.* **245**, 159–166 (2003)
- Martyla, A., Olejnik, B., Kirszensztejn, P., Przekop, R.: Influence of the method of synthesis on hydrogen adsorption properties of mesoporous binary B₂O₃/Al₂O₃ gel systems. *Int. J. Hydrog. Energy.* **36**, 8358–8364 (2011)
- Ward, D.A., Ko, E.I.: Preparing catalytic materials by the sol-gel method. *Ind. Eng. Chem. Res.* **34**, 421–433 (1996)
- Kosmulski, M.: pH-dependent surface charging and points of zero charge. IV. Update and new approach. *J. Colloid Interface Sci.* **337**, 439–448 (2009)
- Narayanan, R., Laine, R.M.: Synthesis of soluble aluminium carboxylates directly from aluminium hydroxide. *J. Mater. Chem.* **10**, 2097–2104 (2000)
- Goodwin, L.F., Sterne, E.T.: Losses incurred in the preparation of acetone by the distillation of acetate of lime. *Ind. Eng. Chem.* **12**, 240–243 (1920)
- Zhang, D., Pan, X., Yu, H., Zhai, Y.: Mineral transition of calcium aluminate clinker during high-temperature sintering with low-lime dosage. *J. Mater. Sci. Technol.* **31**, 1244–1250 (2015)
- Stammore, B.R., Gilot, P.: Review—calcination and carbonation of limestone during thermal cycling for CO₂ sequestration. *Fuel Process. Technol.* **86**, 1707–1743 (2005)
- Sing, K.S.W., Everett, D.H., Haul, R.A.W., Moscou, L., Pierotti, R.A., Rouquerol, J., Siemieniowska, T.: Reporting physisorption data for gas/solid systems with special reference to the determination of surface area and porosity (recommendations 1984). *Pure Appl. Chem.* **57**, 603–619 (1985)
- Imtiaz, A., Farrukh, M.A., Khaleeq-ur-rahman, M., Adnan, R.: Micelle-assisted synthesis of Al₂O₃·CaO nanocatalyst: optical properties and their applications in photodegradation of 2,4,6-trinitrophenol. *Sci. World J.* **2013**, 641420, 11 pages (2013). <https://doi.org/10.1155/2013/641420>
- Pappas, G.S., Liatsi, P., Kartsonakis, I.A., Danilidis, I., Kordas, G.: Synthesis and characterization of new SiO₂–CaO hollow nanospheres by sol–gel method: bioactivity of the new system. *J. Non-Cryst. Solids.* **354**, 755–760 (2008)
- Vázquez, A., López, T., Gómez, R., Bokhimi, Morales, A., Novaro, O.: X-ray diffraction, FTIR, and NMR characterization of sol-gel alumina doped with lanthanum and cerium. *J. Solid State Chem.* **128**, 161–168 (1997)